View metadata, citation and similar papers at core.ac.uk

brought to you by CORE

provided by CURVE/open

Do magnetic fields enhance turbulence at low magnetic Reynolds number?

Potherat, A & Klein, RA

Author post-print (accepted) deposited by Coventry University's Repository

Original citation & hyperlink:
Potherat, A & Klein, RA 2017, 'Do magnetic fields enhance turbulence at low magnetic Reynolds number?' Physical Review Fluids, vol 2, 063702
https://dx.doi.org/10.1103/PhysRevFluids.2.063702

DOI 10.1103/PhysRevFluids.2.063702
ESSN 2469-990X

Publisher: American Physical Society

Copyright © and Moral Rights are retained by the author(s) and/ or other copyright owners. A copy can be downloaded for personal non-commercial research or study, without prior permission or charge. This item cannot be reproduced or quoted extensively from without first obtaining permission in writing from the copyright holder(s). The content must not be changed in any way or sold commercially in any format or medium without the formal permission of the copyright holders.

This document is the author's post-print version, incorporating any revisions agreed during the peer-review process. Some differences between the published version and this version may remain and you are advised to consult the published version if you wish to cite from it.

Do magnetic fields enhance turbulence at low magnetic Reynolds number ?

Alban Pothérat[1,2] and Rico Klein[1]
[1] *Applied Mathematics Research Centre, Coventry University, Priory Street Coventry CV1 5FB, United Kingdom*
[2] *Laboratoire National des Champs Magnétiques Intenses- Grenoble, Université Grenoble-Alpes/CNRS, 25 Rue des Martyrs, B.P. 166 38042 Grenoble Cedex, France* *

arXiv:1511.02364v4 [physics.flu-dyn] 3 Jul 2017

Imposing a magnetic field on a turbulent flow of electrically conducting fluid incurs the Joule effect. A current paradigm is that the corresponding dissipation increases with the intensity of the magnetic field, and as a result turbulent fluctuations are all the more damped as the magnetic field is strong. While this idea finds apparent support in the phenomenology of decaying turbulence, measurements of turbulence in duct flows and other, more complex configurations have produced seemingly contradicting results. The root of the controversy is that magnetic fields promote sufficient scale-dependent anisotropy to profoundly reorganise the structure of turbulence, so their net effect cannot be understood in terms of the additional dissipation only. Here we show that when turbulence is forced in a magnetic field that acts on turbulence itself rather than on the mechanisms that generate it, the field promotes large, nearly 2D structures capturing sufficient energy to offset the loss due to Joule dissipation, with the net effect of increasing the intensity of turbulent fluctuations. This change of paradigm potentially carries important consequences for systems as diverse as the liquid cores of planets, accretion disks and a wide range of metallurgical and nuclear engineering applications.

I. INTRODUCTION

Turbulent flows are often exposed to magnetic fields, either externally applied, or self-generated. In strong mean fields, the induced Lorentz force alters the way flows transport heat or mass, and dissipate energy [32]. Among the vast array of processes that are concerned are the dynamics of liquid planetary cores [30], the solidification of metallic alloys [18, 27], and the cooling of nuclear reactors [33]. The current paradigm is that the action of the field on the flow is a damping one, because of the extra dissipation incurred by the Lorentz force [9]. It finds support in the phenomenology of freely decaying magnetohydrodynamic (MHD) turbulence, which decays faster under a higher externally imposed magnetic field [21, 25]. Nevertheless, the presence of an external magnetic field does not, in general, damp instabilities or turbulent fluctuations. Quite the opposite happens in axisymmetric flows subject to axial and toroidal magnetic fields, where the magnetorotational and Tayler instabilities occur (MRI and TI, respectively). Both instabilities have been theoretically predicted from linear stability analysis [19, 39] but only recently observed in liquid metal experiments [31, 37]. MRI might explain why accretion disks, which should remain laminar in the absence of a magnetic field are in fact turbulent. TI is a good candidate to explain the mechanisms behind the Sun's dynamo [4]. In both cases, the instability mechanisms involve a two-way coupling between the magnetic field and the flow. Yet, enhancement of turbulent fluctuations has been reported in a number of examples where the magnetic field was imposed, and not influenced by the flow too: in numerical simulations and laboratory models for the continuous steel casting process, the complex DC magnetic field applied to control the flow was found to drive high amplitude turbulent fluctuations [8, 20, 40]. The picture is more complex in duct flows subject to an imposed magnetic field: when the flow is driven by pressure alone, the intensity of turbulent fluctuations decreases in the central part of the duct at higher magnetic fields [17]. By contrast, earlier experiments clearly show an increase in turbulent intensity with an external magnetic field in duct flows where turbulence is generated by a grid [11, 16, 38], or in numerically forced flows in periodic domains [5]. In pressure-driven duct flows, turbulence is produced by shear layer instabilities, which are severely damped by the magnetic field, so [17] arguably confirms that the magnetic field damps this particular mechanism of turbulence production [6]. However, the question of the effect of magnetic fields on turbulence itself remains open and needs to be addressed in conditions where it is not overshadowed by the magnetic field's influence on the mechanism forcing turbulence.

We tackle this problem by considering a generic plane channel geometry pervaded by a uniform magnetic field perpendicular to it. We assume that (i) that the flow is driven by an external force that is not affected by the magnetic field and (ii) the magnetic field induced by the flow is sufficiently small for the externally applied magnetic field $\mathbf{B}$ to be considered constant, *i.e.* that the magnetic Reynolds number is small [29]. This approximation applies to most laboratory experiments with flows of moderate intensity. The key mechanism at play in these conditions was first characterised by the authors of Ref. [36], who showed that in inducing eddy currents to oppose velocity gradients along the magnetic field, the Lorentz force diffuses momentum along $\mathbf{B}$

* alban.potherat@coventry.ac.uk

over a timescale $\tau = \tau_J(l_z/l_\perp)^2$. Here, $\tau_J = \rho/(\sigma B^2)$ is the Joule dissipation time, $l_\perp$ and l_z are lengthscales across and along the field, σ and ρ are the fluid's electrical conductivity and density. In turbulent flows, diffusion is disrupted by inertial transfer acting over a structure turnover time $\tau_U \sim l_\perp/U(l_\perp)$, where $U(l_\perp)$ is a typical velocity at scale $l_\perp$. The competition between both processes determines the scale-dependent anisotropy as $l_z(l_\perp) \sim l_\perp N(l_\perp)^{1/2}$, $N(l_\perp) = \tau_U/\tau_J$ being the interaction parameter at scale $l_\perp$ (see the theory from Ref. [36] and experimental evidence in Ref. [24]). As a result of this process, velocity gradients are reduced under the action of the magnetic field as $\partial_z \sim l_z^{-1} \propto B^{-1}$, and so is the current density. In a channel of width h, perpendicular to the magnetic field, the flow dimensionality is therefore determined by the scale-dependent ratio $l_z(l_\perp)/h$ [24]: if $l_z(l_\perp)/h < 1$ a structure of size $l_\perp$ is 3D. In the limit $l_z(l_\perp)/h \to \infty$, it is quasi-2D. In the quasi-2D limit, no eddy currents remain in the bulk, because diffusion then takes place across the entire channel, except in Hartmann boundary layers along the channel walls [22]. Current that would be directly induced in the bulk by an external force (through Lenz's law) returns through the Hartmann layers too. All three cases are illustrated in Fig. 1.

To understand how this effect determines the intensity of turbulence, we shall first translate this phenomenology into a scaling linking the relative turbulent intensity with the forcing and magnetic field intensities (section II). Second, we shall experimentally drive turbulence in a liquid metal experiment where the forcing intensity can be precisely set, and measure both relative and absolute turbulent intensities (section III).

II. THEORY

A. Scaling for the local, event-averaged Reynolds number.

We consider the generic configuration of an electrically conducting fluid (density ρ, electric conductivity σ, and viscosity ν) confined between two parallel walls distant by h and pervaded by a uniform magnetic field $\mathbf{B} = B\mathbf{e}_z$ normal to them. The flow is driven by an external force density field $\mathbf{F}$ non-dimensionally measured by the Grashof number $\mathcal{G} = Fl_\perp^3/(\rho\nu^2)$, where $l_\perp$ is a lengthscale perpendicular to $\mathbf{e}_z$ (Fig. 1). For simplicity, $\mathbf{F}$ is chosen normal to $\mathbf{e}_z$. The first step is to seek a scaling for the average flow intensity for a given external force and magnetic field. Away from the wall, $\mathbf{F}$ is balanced by inertia and the Lorentz force. At low magnetic Reynolds numbers, magnetic field fluctuations are negligible compared to the externally imposed field [29]; the governing equations can be expressed in the form of the incompressible Navier-Stokes equations with an added term representing the Lorentz force density $\mathbf{J}\times\mathbf{B}$ and the constraints that the velocity field $\mathbf{u}$ and current density field $\mathbf{J}$ must be solenoidal to ensure mass and charge conservation.

$$(\partial_t + \mathbf{u}\cdot\nabla)\mathbf{u} + \frac{1}{\rho}\nabla p = \nu\Delta\mathbf{u} + \frac{1}{\rho}\mathbf{J}\times\mathbf{B} + \frac{1}{\rho}\mathbf{F}, \quad (1)$$

$$\nabla\cdot\mathbf{u} = 0, \quad \nabla\cdot\mathbf{J} = 0. \quad (2)$$

The system is closed with the addition of Ohm's law

$$\frac{1}{\sigma}\mathbf{J} = -\nabla\phi + \mathbf{u}\times\mathbf{B}, \quad (3)$$

where ϕ is the electric potential. Away from the walls, the curl of the Navier-Stokes equations and charge conservation yield the gradient of current density J_z along z [24]:

$$-\partial_z J_z = \frac{1}{B}\left[-\rho\nabla\times(\mathbf{u}\cdot\nabla)\,\mathbf{u} + \nabla\times\mathbf{F}\right]\cdot\mathbf{e}_z. \quad (4)$$

Equation (4) expresses that horizontally divergent eddy currents (*lhs.*) are induced by the rotational part of the forcing (second term, *rhs.*). Part of them returns through the bulk where the Lorentz force they induce balances inertia (first term, *rhs.*). Consider a structure of size $l_\perp$ and velocity U extending over height h_V along the magnetic field. From Eq. (4) the total current generated by the forcing inside the structure and following this path scales as $I_B \sim (\pi\rho l_\perp^2 h_V/B)(U^2/l_\perp^2)$, and the current induced by the forcing scales as $I_F \sim (\pi\rho l_\perp^2 h_V/B)(F/\rho l_\perp)$. The remaining current I_H (*lhs.* of (4)) returns through the thin Hartmann boundary layers that develop along the walls [22]. The Lorentz force they generate there is opposed by viscous friction only (see Fig. 1). This balance determines the thickness $\delta_H = B^{-1}(\rho\nu/\sigma)^{1/2}$ of these layers and the current density flowing through them $J_H \sim \sigma BU$ [22]. Consequently, the total current through the Hartmann layer scales as $I_H \sim 2\pi l_\perp J_H \delta_H$. From this phenomenology, Eq. (4) reduces to the conservation of the global current induced by the forcing $I_F = I_H + I_B$, and from the scalings for each term, Eq.(4) is expressed non-dimensionally as

$$\mathcal{G} - Re^2 \sim 2\frac{h}{h_V}\left(\frac{l_\perp}{h}\right)^2 HaRe, \quad (5)$$

where $Re = Ul_\perp/nu$ is the Reynolds number, and the Hartmann number $Ha = h/\delta_H$ provides a non-dimensional measure of $\mathbf{B}$.

The height h_V of the structure in the bulk is determined by the anisotropic action of the Lorentz force as follows: In the limit $Re/Ha \gg 1$, the bulk of the flow is 3D, and h_V is set by the momentum diffusion length defined in the introduction $h_V \sim l_z(l_\perp)$. In this case, inertia in the bulk consumes the larger part of the current induced by external forcing, so it remains from (5) that

$$Re \sim \mathcal{G}^{1/2}. \quad (6)$$

Since the contribution of the Hartmann layers in (5) is small in this limit, Eq. (6) remains valid whether

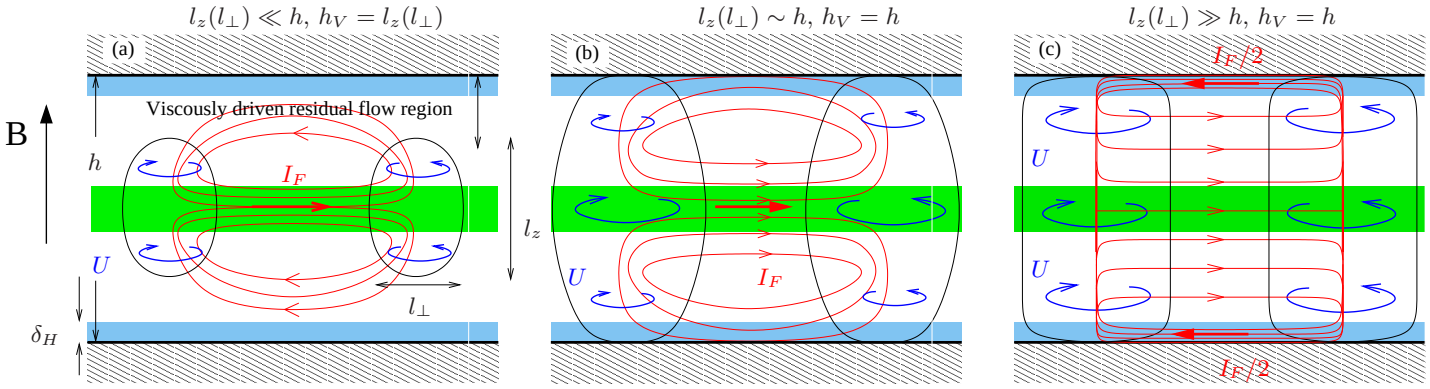

FIG. 1. Generic flow structures of lengthscale $l_\perp$ driven by an external force $\mathbf{F}$ (in the green area) in an external magnetic field $\mathbf{B}$. The Lorentz force diffuses momentum along the field over $l_z(l_\perp)$, and induces electric currents (in red). (a) $l_z(l_\perp) \ll h$: the current driven by the external forcing returns in the bulk. Only a residual flow exists near the walls. (b) $l_z(l_\perp) \sim h$: the current returns in the bulk and the Hartmann layers (in blue): the flow is still 3D but influenced by the walls. (c) $l_z(l_\perp) \gg h$: the current returns equally in the top and bottom Hartmann layers, and not in the bulk: the flow is quasi-2D.

or not the flow interacts with the walls (in this latter case the current induced by the forcing returns entirely over height l_z, determined by the balance between the Lorentz force and inertia (*i.e.* $I_H = 0$, as in Fig. 1-(a)). Experiments on electrically driven turbulence (See Fig. 4-a in Ref. [24]) showed that this relation holds to a great precision for turbulent flows, if the Reynolds number $Re = \langle|\mathbf{u}|\rangle L_f/\nu$ is expressed in terms of the average velocity in the forced region and the forcing lengthscale L_f (*i.e* by setting $l_\perp = L_f$ and $U = \langle|\mathbf{u}|\rangle$ in the derivation above). Even for Ha up to 2×10^4, the left hand side correction in (5) due to current circulating in the Hartmann layers remained small, which confirms the validity of (6).

B. Scaling relation for the relative turbulent intensity.

We shall now seek an estimate for the turbulent intensity, for given control parameters $\mathcal{G}$ and Ha, *i.e* for given forcing and magnetic fields. For this, we first note that unlike in hydrodynamic turbulence, dissipation in MHD turbulence is Ohmic and roughly scales as $\epsilon_J \sim (\nu/h^2) Ha^2 \|\mathbf{u}\|^2 (l_\perp/l_z)^2$ (a more precise scaling will be obtained in this section). Consequently, it preferentially affects large scales exhibiting three-dimensionality (*i.e* for which l_z remains finite). Hence, the tendency toward two-dimensionality of MHD turbulence, which is a by-product of the dissipative process, is independent of its spectral structure [13] and the global dissipation can be captured by means of a power budget over a volume V of height h along $\mathbf{B}$ and size $l_\perp$ greater than the forcing scale. Decomposing the velocity field $\mathbf{u} = \langle\mathbf{u}\rangle + \langle\mathbf{u}'^2\rangle^{1/2}$ into average and fluctuations, we shall write this budget separating the current density field $\mathbf{J}$ into its average and fluctuating parts returning through the Hartmann layers $\langle\mathbf{J}_{2D}\rangle + \mathbf{J}'_{2D}$ and its average and fluctuating parts returning through the bulk $\langle\mathbf{J}_{3D}\rangle + \mathbf{J}'_{3D}$:

$$\Big\langle \int_V \mathbf{F}\cdot\langle\mathbf{u}\rangle + (\langle\mathbf{J}_{3D}\rangle + \mathbf{J}'_{3D} + \langle\mathbf{J}_{2D}\rangle + \mathbf{J}'_{2D}) \times \mathbf{B}\cdot(\langle\mathbf{u}\rangle + \mathbf{u}') + \rho\nu\,(\langle\mathbf{u}\rangle + \mathbf{u}')\cdot\Delta\,(\langle\mathbf{u}\rangle + \mathbf{u}')\,dV\Big\rangle = 0, \tag{7}$$

This way, the budget reflects the structure of the eddy currents identified previously: The power $\mathcal{P}_F$ generated by the forcing is consumed in three ways: Joule dissipation due to current returning through the bulk ϵ_{3D}, Joule dissipation due to currents returning through the Hartmann layers ϵ_{2D}, and viscous dissipation ϵ_ν almost entirely produced in the Hartmann layers:

$$\mathcal{P}_F + \epsilon_J^{3D} + \epsilon_J^{2D} + \epsilon_\nu = 0. \tag{8}$$

The contribution from inertial and pressure terms is neglected on the grounds that it is $N(l_\perp)$ times smaller than Joule dissipation and that for strong enough magnetic fields, $N(l_\perp) \gg 1$. This condition sets a minimum lengthscale $l_\perp$ for Eq. (8) to be valid over $V(l_\perp)$. The forcing power is evaluated by noticing that eddy currents induced by the forcing diffuse over the lengthscale $l_z(l_\perp)$ built on the average velocity:

$$\mathcal{P}_F \sim l_\perp^2 l_z(l_\perp) |\langle\mathbf{u}\rangle| |\mathbf{F}| \sim \rho\nu h \langle\mathbf{u}\rangle^2 \mathcal{G} Ha Re^{-3/2}. \tag{9}$$

Joule dissipation in the bulk can be related to the velocity field by virtue of the expression of the rotational part of Lorentz force put forward by [36]:

$$[\mathbf{J}\times\mathbf{B}]_{\nabla\times} = -\frac{\rho}{\tau_J}\Delta^{-1}\partial_{zz}^2\mathbf{u}. \tag{10}$$

Since bulk velocity gradients along the magnetic fields are controlled by the diffusion of momentum by the Lorentz force, $\Delta^{-1}\partial_{zz}^2 \sim (l_\perp/l_z)^2$. Importantly, however, mean flow and fluctuations may significantly differ in intensity and may therefore diffuse over different

lengths under the action of the Lorentz force, respectively $l_z = l_\perp N(|\langle \mathbf{u}\rangle|)^{1/2}$ and $l'_z = l_\perp N(\langle \mathbf{u'}^2\rangle^{1/2})^{1/2}$. Hence, separating average and fluctuating parts yields:

$$\epsilon_J^{3D} = -\frac{\rho}{\tau_J}\int_V \left[\langle \mathbf{u}\rangle \cdot \Delta^{-1}\partial_{zz}^2\langle \mathbf{u}\rangle + \langle \mathbf{u'}\cdot\Delta^{-1}\partial_{zz}^2\mathbf{u'}\rangle\right] dV, \\ \sim \rho\nu h\langle \mathbf{u}\rangle^2 Re(1+\alpha^3), \tag{11}$$

where

$$\alpha = \langle \mathbf{u'}^2\rangle^{1/2}/|\langle \mathbf{u}\rangle| \tag{12}$$

is the relative turbulent intensity.
Dissipation in the Hartmann layers is equally Ohmic and viscous $\epsilon_J^{2D} = \int_V(\langle \mathbf{J}_{2D}\rangle + \mathbf{J}'_{2D}) \times \mathbf{B}\cdot\mathbf{u}dV \simeq \epsilon_\nu = \int_V \rho\nu\mathbf{u}\cdot\Delta\mathbf{u}dV \simeq \int_V \rho\nu\mathbf{u}\cdot\partial_{zz}^2\mathbf{u}dV$ and is estimated from the thickness of the Hartmann layer $\delta_H = h/Ha$ [22]:

$$\epsilon_J^{2D} \simeq \epsilon_\nu \sim -\rho\nu h\langle \mathbf{u}\rangle^2\left(\frac{l_\perp}{h}\right)^2 Ha(1+\alpha^2). \tag{13}$$

By virtue of (9,11,13), and (7) becomes

$$\mathcal{G}HaRe^{-1/2}\left(\frac{l_\perp}{h}\right) \sim Re^2(1+\alpha^3)+2HaRe\left(\frac{l_\perp}{h}\right)^2(1+\alpha^2). \tag{14}$$

Lastly, Re, which is not known *a priori*, is expressed in terms of control parameter $\mathcal{G}$ through scaling (6). This yields a simplified relation linking the relative turbulent intensity α to control parameters Ha and $\mathcal{G}$:

$$Ha\mathcal{G}^{-1/4}\left(\frac{l_\perp}{h}\right) \sim (1+\alpha^3) + 2Ha\mathcal{G}^{-1/2}\left(\frac{l_\perp}{h}\right)^2(1+\alpha^2). \tag{15}$$

These estimates reflect that increasing B (or Ha) extends the thickness of the forced region by $l_z \propto B$. Consequently, the forcing power increases linearly with B. On the other hand, the power dissipated in the bulk does not vary with B because the intensity of the eddy currents there is governed by velocity gradients along z that decrease as $l_z^{-1} \propto B^{-1}$, thus exactly compensating the increase in B. Plots of (15) in Fig. 3 show that the relative intensity of turbulence increases with the externally imposed magnetic field (or Ha), with $\alpha \propto Ha^{1/3}$ for $\alpha > 1$. The underlying phenomenology reflects anisotropic mechanisms that are the hallmark of MHD turbulence: in 3D flows, high velocity gradients along the magnetic field incur Joule dissipation that damps velocity fluctuations. As the magnetic field increases, turbulent structures elongate as $l'_z(l_\perp)$ increases, velocity gradients weaken, so does the Joule dissipation they incur, and turbulent fluctuations retain more energy. Through this process, the relative intensity of turbulent fluctuations is higher for higher magnetic fields.

III. EXPERIMENTS

A. Experimental approach.

Our second step is to test scaling relation (15) on the FLOWCUBE facility, which reproduces the generic configuration from Fig. 1 in a 10 cm-cubic vessel filled with liquid metal pervaded by the near-homogeneous magnetic field generated in the bore of a superconducting solenoidal magnet. The metal is Gallinstan, an eutectic alloy of gallium, indium and tin that is liquid a room temperature. Full details and validation of the experimental setup are provided in [3, 24]. An electrically generated force of lengthscale L_f keeps turbulence in a statistically steady state as follows: Electric current I locally injected through one of the channel walls (arbitrarily the bottom wall) forces horizontally divergent currents through the bulk and the Hartmann layers. Their interaction with the externally imposed magnetic field exerts a driving Lorentz force on the flow. This mechanism ensures that the forcing is directly controlled by the injected current and does not vary with the external magnetic field. This somewhat counter-intuitive result comes as a consequence of the diffusion by the Lorentz force over $l_z \sim L_f N^{1/2} = L_f Ha/Re^{1/2}(L_f/h)$ of the current I injected through the wall. Because of this effect, the volume of forced fluid increases linearly with the magnetic field. Hence, the horizontal current density driving fluid motion scales as $J_\perp \sim I/(2\pi L_f l_z)$. It follows that the force density driving turbulence is controlled by the injected current I only, as $F \sim IB/(2\pi L_f l_z) = I(\rho\nu/\sigma)^{1/2}/(2\pi L_f^3)Re^{1/2}$, and does not depend on the magnetic field. By virtue of (6), $\mathcal{G} = [I/(2\pi(\nu^3\sigma\rho)^{1/2})]^{4/3}$ is varied solely by adjusting the injected current I. This method can be understood as an extension to 3D turbulence of the method of [35] to force quasi-2D MHD flows, where the forcing was also controlled by the current measured non-dimensionally by the parameter

$$Re_0 = \frac{I}{2\pi(\sigma\rho\nu^3)^{1/2}} = \mathcal{G}^{3/4}. \tag{16}$$

Based on this principle, turbulence is driven in FLOWCUBE by injecting current through electrodes embedded flush in the bottom wall, arranged in a 10×10 square array of step $L_f = 1$ cm and alternately connected to the positive and negative poles of a DC current supply. The corresponding average flow is a crystal of columnar vortices attached to the bottom wall extending by $l_z(L_f)$ into the bulk through diffusion by the Lorentz force (see [14, 24] for a detailed analysis of this flow, and [2, 23, 26] for a theory explaining how its componentality is controlled by the magnetic field). The region just outside the bottom Hartmann layer is always in the forcing region and is representative of the bulk of forced turbulence. On the other hand, the region just outside of the Hartmann layer near the top wall may lay within the forcing region if $l_z(L_f)/h = N(L_f)^{1/2}L_f/h > 1$ or outside it

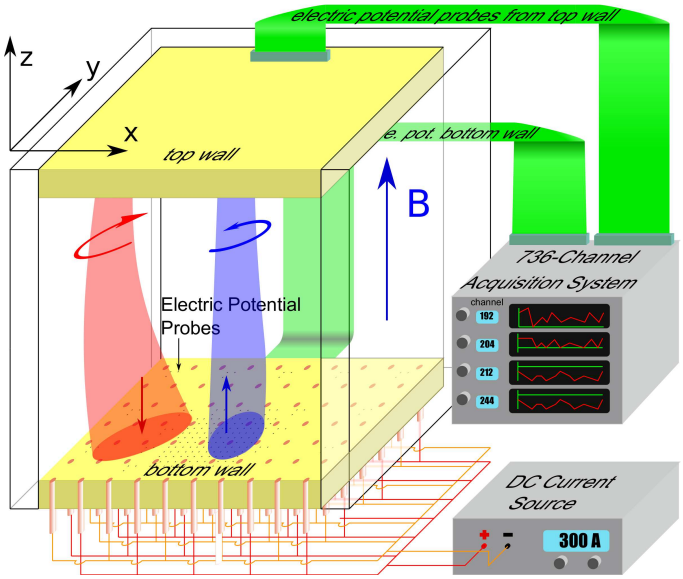

FIG. 2. Simplified sketch of the FLOWCUBE platform for the study of electrically driven liquid metal flows representing the main vessel filled with liquid metal with Hartmann walls (in yellow) and walls parallel to the magnetic field (transparent). The flow is forced by injecting DC electric current through a square array of electrodes embedded flush in the bottom wall. This creates a crystal of columnar vortices, which in destabilising, gives rise to turbulence. An external magnetic field is applied by means of a large solenoidal cryomagnet (not represented). Depending on the intensities of the magnetic field and turbulence, turbulence extends to part of the bulk (if $l'_z(L_f) < h$) or up to the top wall (if $l'_z(L_f) \gtrsim h$). Velocities are reconstructed just outside the boundary layers near the top and bottom walls, from measurements of electric potential at 384 contact probes embedded flush in the top and bottom walls (black dots) and connected to a 768-channel, high precision acquisition system through printed circuit built-in the Hartmann walls.

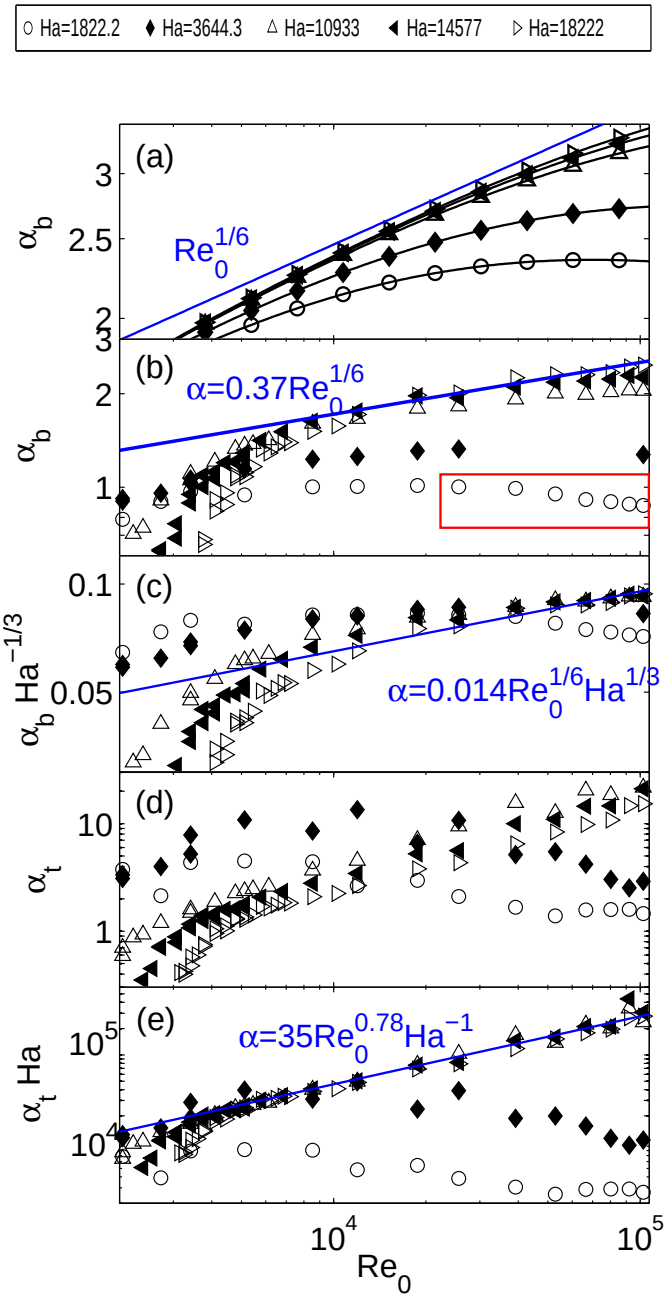

FIG. 3. Relative turbulent intensity near the bottom wall (forced region) (from (a) Eq. (15), (b,c): experiment) and (d) top wall, $\alpha_{b,t} = \langle \mathbf{u}'^2_{b,t} \rangle^{1/2} / |\langle \mathbf{u}_{b,t} \rangle|$. The red rectangle indicates the regime of strongest three-dimensionality, where turbulent fluctuations increase with the external magnetic field and decrease as $\mathcal{G}^{-1/12}$ with the forcing. The slope $Re_0^{1/6} (\propto \mathcal{G}^{1/8})$ is indicative only, as the solution of (15) for $\alpha(\mathcal{G})$ is not a power law.

if $l_z(L_f)/h < 1$. Since L_f is the scale of the average flow, Re, N and $\mathcal{G}$ are evaluated taking $l_\perp = L_f$. As in Section II, we shall distinguish between N and N', built on the average velocity and the fluctuations, respectively.
Bulk velocities are measured locally just outside the bottom and top Hartmann layers by electric potential velocimetry [15] through 192 electric potential probes fitted flush in each of the Hartmann walls [24]. Average and RMS fluctuations near bottom and top walls (denoted by indices $_b$ and $_t$ respectively) are obtained from spatial and time averages of time-dependent signals of $\mathbf{u}_{b,t}(x, y, t)$, recorded in a statistically state.

B. Relative turbulent intensity.

Relative turbulent intensities near the bottom and top walls $\alpha_{b,t} = \langle \mathbf{u}'^2_{b,t} \rangle^{1/2} / |\langle \mathbf{u}_{b,t} \rangle|$ are shown in Fig. 3. Within the forced region of the flow (*i.e.* near the bottom

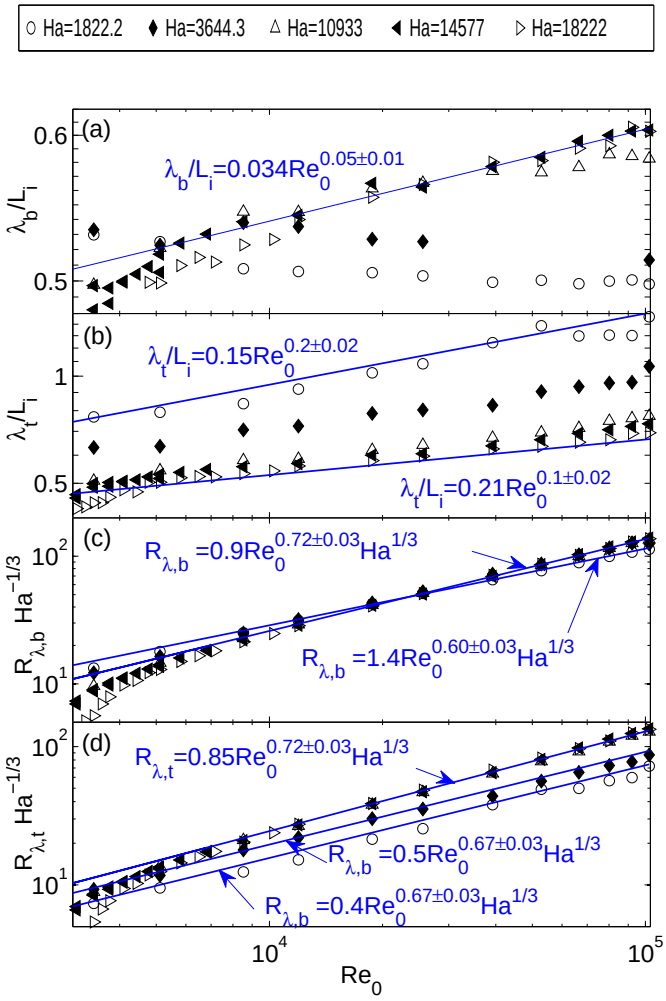

FIG. 4. Taylor microscale near (a) the bottom wall (λ_b, forced region), and (b) the top wall (λ_t, outside the forced region if $l_z(L_f) > h$), and Reynolds number R_λ based on (c) λ_b and (d) λ_t, showing increasing absolute turbulent intensity with the external magnetic field both within and outside the forced region.

wall, see Fig. 3-b), α_b is found to always increase with Ha and its variations are very well reproduced by the scaling relation (15): in both theory and experiments, $\alpha_b \propto Ha^{1/3}$ for $\alpha_b > 1$, a regime where both the top and the bottom walls lie within the forced region (*i.e* $l_z(L_f) > h$). When $\alpha_b \lesssim 1$, the dependence on Ha is even stronger than $Ha^{1/3}$. In this regime, $l_z(L_f) < h$ so the forcing region progressively extends across the channel as Ha is increased. The increase in actual vortex length along $\mathbf{B}$ causes a drastic reduction of velocity gradients along z and a drop in bulk dissipation that translates into the sharper increase of turbulent fluctuations observed.

Equation (15) and its underlying phenomenology are further validated in the most 3D regimes ($Ha = 1822$, high $\mathcal{G}$), where α_b decreases with $\mathcal{G}$ (Region inside the red rectangle in Fig. 3-b). This behaviour is captured in the limit where Joule dissipation mostly occurs in the bulk, in which case (15) reduces to $\alpha_b \propto \mathcal{G}^{-1/12} \propto Re_0^{-1/9}$.

By contrast Eq. (15) does not apply to relative fluctuations α_t near the top wall, which lays outside the forced region if $l_z(L_f) \lesssim h$. Indeed relative turbulent fluctuations there first sharply increase with Ha for $Ha < 7500$ as large scale fluctuations diffuse up when Ha increases, to progressively reach the top wall. Fluctuations then decrease slightly with Ha: rather than a loss of intensity in turbulence, we shall see that this reflects an increasing intensity of the mean flow near the top wall.

C. Absolute turbulent intensity.

To isolate the influence of the magnetic field on turbulent fluctuations from that on the mean flow, absolute turbulent intensity was measured through the microscale Reynolds number

$$R_{\lambda,b,t} = \langle \mathbf{u}'^2_{b,t} \rangle^{1/2} \lambda_{b,t}/\nu, \tag{17}$$

based on the Taylor microscale

$$\lambda_{b,t} = \left[\frac{\langle \mathbf{u}'_{b,t}(\mathbf{x}) \cdot \mathbf{u}'_{b,t}(\mathbf{x}+\mathbf{r}) \rangle}{\partial^2_{rr} \langle \mathbf{u}'_{b,t}(\mathbf{x}) \cdot \mathbf{u}'_{b,t}(\mathbf{x}+\mathbf{r}) \rangle} \right]^{1/2} (\mathbf{r}=0), \tag{18}$$

which is representative of the inertial range of turbulence [12]. The variations of λ near the bottom (λ_b, Fig. 4-a) and top walls (λ_t, Fig. 4-b) turn out to be very weak. Hence, the variations of R_λ are driven by the velocity fluctuations. Just like the relative turbulent intensity, the microscale Reynolds number (Figs. 4-c and 4-d) follows a scaling of $R_{\lambda,b,t} \propto Ha^{1/3}$ in the limit of high Ha. There are, however, two important differences. First, unlike relative fluctuations, absolute fluctuations always increase with Ha, both inside and outside the forcing region. Second, they always increase with the forcing too, confirming that the decrease in relative turbulent intensity with either the forcing (for low Ha) or the magnetic field outside the forcing region reflects an intensification of the average flow, and not weakening turbulent fluctuations.

IV. DISCUSSION.

These results provide robust evidence that the intensity of forced MHD turbulence increases with an externally applied magnetic field, when the forcing density is kept constant and when the damping of energy transfer from mean flow to turbulence by the magnetic field does not mask its influence on turbulence itself. In the FLOWCUBE setup, constant forcing density is obtained by driving turbulence with a constant electric current but

the same result can be achieved with other types of forcing mechanisms: If the flow had been locally forced by means of a propeller, since the forced volume increases as $l_z(L_f) \propto B$, the total torque on the propeller would have to increase with B to keep the force density constant over the entire forced volume. Regardless of the forcing mechanism, in any given volume of forced turbulence, velocity gradients along the field are smoothed out by the Lorentz force as the field increases. This mechanism reduces Joule dissipation. It allows turbulent fluctuations to retain more energy, and thereby leads turbulent intensity to increase as the magnetic field is increased. In grid turbulence experiments [1, 11, 16, 38], the average fluid velocity relative to the grid was kept constant. This impled increasing the driving force with the magnetic field to overcome the obstacle resistance. Equation (6) implies that keeping the average velocity constant is indeed equivalent to keeping the force density constant, so the phenomenology identified in the FLOWCUBE applies to these experiments on duct flows too. Indeed, [11] shows an increase of approximately $\alpha \propto B^{0.5\pm0.1}$ for $Ha \gtrsim 10^3$, which is consistent with our own findings at low values of Ha. Hence, while magnetic fields may damp instabilities in duct flows, they enhance turbulent fluctuations in general, in duct flows and other configurations. This phenomenon stems from the promotion of larger, more two-dimensional scales at higher magnetic fields. The higher the fields, the wider the range of quasi-2D scales and the more intense the turbulent fluctuations. This mechanism is further reinforced as large quasi-2D scales promote an inverse energy cascade that channels the energy injected by the forcing to them [10, 28, 34].

In our experiment, the forcing, rather than turbulent production itself was kept constant and independent of the field. Hence, the increase in turbulent intensity took place despite a possible loss in the energy transferred from the mean flow to turbulence. A more precise characterisation of turbulence enhancement would be obtained by holding turbulent production constant, which can be envisaged in numerical simulations, rather than experiments.

An important point to notice is that the reduction of velocity gradients with increasing magnetic field is the core effect driving turbulence enhancement. As a direct consequence, this mechanism cannot act when both the average flow and fluctuations cease to exhibit any gradients along the magnetic field, *i.e.* when all flow structures are quasi-2D (as on Fig. 1-(c)). Such a regime is not reached in FLOWCUBE for the magnetic fields considered here. However, [11] precisely reports a decrease in turbulent intensity with the fluctuations in the quasi-2D regime, which provides further support of the turbulence enhancement scenario we put forward.

Finally, two-dimensionalisation and energy cascades toward large scales exist in other systems. For example, rotation promotes less dissipative quasi-2D turbulence too, as the Coriolis force plays a similar role to that of the Lorentz force in MHD turbulence [7]. Hence, it can be expected that the intensity of turbulent fluctuations should increase with rotation too, as unlike the Lorentz force, the Coriolis force generates no dissipation to oppose this mechanism.

ACKNOWLEDGMENTS

A. Pothérat acknowledges support from the Royal Society under the Wolfson Research Merit Award scheme (Grant No. WM140032) and the International Exchanges scheme (Grant No. IE140127), from Université Grenoble Alpes and from Grenoble INP for the invited Professor positions they have granted him during the course of this project.

[1] A. Alemany, R. Moreau, P. Sulem, and U. Frish. Influence of an external magnetic field on homogeneous MHD turbulence. *J. Mec.*, 18(2):277–313, 1979.

[2] N. Baker, A. Pothérat, and L. Davoust. Dimensionality, secondary flows and helicity in Low-*Rm* MHD vortices. *J. Fluid Mech.*, 779:325–350, 2015.

[3] N Baker, A. Pothérat, L. Davoust, F. Debray, and R. Klein. Controlling the dimensionality of low-Rm MHD turbulence experimentally. *Exp. Fluids*, 58(7):79, 2017.

[4] S.A. Balbus and J.F. Hawley. Instability, turbulence, and enhanced transport in accretion disks. *Rev. Mod. Phys.*, 70(1):1–53, 1998.

[5] T. Boeck, D. Krasnov, and A. Thess. Large-scale intermittency of liquid-metal channel flow in a magnetic field. *Phys. Rev. Lett.*, 101:244501, 2008.

[6] T. Boeck, D. Krasnov, O. Zikanov, and M. Rossi. Optimal linear growth in magnetohydrodynamic duct flow. *J. Fluid Mech.*, 653:273–299, 2010.

[7] C. Cambon, N. N. Mansour, and Godeferd. F. S. Energy transfer in rotating turbulence. *J. Fluid Mech.*, 337:303–332, 1997.

[8] R. Chaudhary, B. G. Thomas, and S.P. Vanka. Effect of electromagnetic ruler braking (EMBr) on transient turbulent flow in continuous slab casting using large eddy simulations. *Metall. Materi. Trans. B*, 43(3):532–553, 2012.

[9] P.A.D. Davidson. Magnetohydrodynamics in material processing. *Annu. Rev. Fluid Mech.*, 131:273–300, 1999.

[10] E. Deusebio, Boffetta G., E. Lindborg, and S. Musacchio. Dimensional transition in rotating turbulence. *Phys. Rev. E*, 90:023005, 2014.

[11] S Eckert, G Gerbeth, W Witke, and H Langenbrunner. MHD turbulence measurements in a sodium channel exposed to a transverse magnetic field. *Int. J. Heat Fluid Flow*, (22):358–364, 2001.

[12] U. Frisch. *Turbulence, The Legacy of A.N. Kolmogorov.* Cambridge University Press, Cambridge, 1995.

[13] B. Gallet and C. R. Doering. Exact two-dimensionalization of low-magnetic-Reynolds-number flows subject to a strong magnetic field. *J. Fluid Mech.*, 773:154–177, 2015.

[14] R. Klein and A. Pothérat. Appearance of three-dimensionality in wall bounded MHD flows. *Phys. Rev. Lett.*, 104(3):034502, 2010.

[15] A. Kljukin and A. Thess. Direct measurement of the stream-function in a quasi-two-dimensional liquid metal flow. *Exp. Fluids*, 25:298–304, 1998.

[16] Y. B. Kolesnikov and A. B. Tsinober. Experimental investigation of two-dimensional turbulence behind a grid. *Izv. Akad. Nauk. SSSR, Mekh. Zhidk. Gaza. (No. 4)*, 4:146–150 (in Russian), 1974.

[17] D. Krasnov, O. Zikanov, and T. Boeck. Numerical study of magnetohydrodynamic duct flow at high Reynolds and Hartmann numbers. *J. Fluid Mech.*, 704:421–446, 2012.

[18] X. Li, Y. Fautrelle, and Z. Ren. Influence of thermoelectric effects on the solid-liquid interface shape and cellular morphology in the mushy zone during the directional solidification of Al-Cu alloys under a magnetic field. *Acta Materialia*, 55(11):3803–3813, 2007.

[19] W. Liu, J. Goodman, H. Isom, and H. Ji. Helical magnetorotational instability in magnetized Taylor-Couette flow. *Phys. Rev. E*, 74:056302, 2006.

[20] X. Miao, K. Timmel, D. Lucas, Z. Ren, S Eckert, and G. Gerbeth. Effect of an electromagnetic brake on the turbulent melt flow in a continuous-casting mold. *Metall. Materi. Trans. B*, 43(1):954–972, 2012.

[21] H. K. Moffatt. On the suppression of turbulence by a uniform magnetic field. *J. Fluid Mech.*, 28:571–592, 1967.

[22] R. Moreau. *Magnetohydrodynamics*. Kluwer, Dordrecht, 1990.

[23] A. Pothérat. Three-dimensionality in quasi-two dimensional flows: Recirculations and barrel effects. *EPL (Europhys. Lett.)*, 98(6):64003 (6 pages), 2012.

[24] A. Pothérat and R. Klein. Why, how and when MHD turbulence at low Rm becomes three-dimensional. *J. Fluid Mech.*, 761:168–205, 2014.

[25] A. Pothérat and K. Kornet. The decay of wall-bounded MHD turbulence at low *Rm*. *J. Fluid Mech.*, 783:605–636, 2015.

[26] A Pothérat, F Rubiconi, Y. Charles, and V Dousset. Direct and inverse pumping in flows with homogenenous and non-homogenous swirl. *Eur. Phys. J. E*, 36(8):94, 2013.

[27] Prescott, P.J., and F.P Incropera. Effect of turbulence on solidification of a binary metal alloy with electromagnetic stirring. *J. Heat Transfer*, 117(3):716–724, 1995.

[28] S. Reddy and M. K. Verma. Strong anisotropy in quasi-static magnetohydrodynamic turbulence for high interaction parameters. *Phys. Fluids*, 26:025102, 2014.

[29] P. H. Roberts. *Introduction to Magnetohydrodynamics*. Longman, London, 1967.

[30] D. Ryan and G. Sarson "Are geomagnetic field reversals controlled by turbulence within the Earth's core? *Geophys. Res. Lett.*, 34, 2007.

[31] M. Seilmayer, F. Stefani, T. Gundrum, T. Weier, G. Gerbeth, M. Gellert, and G. Rüdiger. Experimental evidence for a transient Tayler instability in a cylindrical liquid-metal column. *Phys. Rev. Lett.*, 108:244501, 2012.

[32] J. V. Shebalin, W. H. Matthaeus, and D. Montgomery. Anisotropy in MHD turbulence due to a mean magnetic field. *J. Plasma Phys.*, 29(3):525–547, 1983.

[33] S. Smolentsev, R. Moreau, and M. Abdou. Characterization of key magnetohydrodynamic phenomena in PbLi flows for the US DCLL blanket. *Fusion Eng. Des.*, 83(5-6):771–783, 2008.

[34] J. Sommeria. Experimental study of the two-dimensionnal inverse energy cascade in a square box. *J. Fluid Mech.*, 170:139–168, 1986.

[35] J. Sommeria. Electrically driven vortices in a strong magnetic field. *J. Fluid Mech.*, 189:553–569, 1988.

[36] J. Sommeria and R. Moreau. Why, how and when MHD turbulence becomes two-dimensional. *J. Fluid Mech.*, 118:507–518, 1982.

[37] F. Stefani, T. Gundrum, G. Gerbeth, G. Rüdiger, M. Schultz, J. Szklarski, and R. Hollerbach. Experimental evidence for magnetorotational instability in a Taylor-Couette flow under the influence of a helical magnetic field. *Phys. Rev. Lett.*, 97:84502, 2006.

[38] S. Sukoriansky, I. Zilberman, and H. Branover. Exerimental studies of turbulence in mercury flows with transverse magnetic field. *Exp. Fluids*, 4(1):11–16, 1986.

[39] R.F. Tayler. The adiabatic stability of stars contaning magnetic fields - I toroidal fields. *Mon. Not. R. Astron. Soc.*, 161(1):365–380, 1973.

[40] K. Timmel, S. Eckert, and G Gerbeth. Experimental investigation of the flow in a continuous-casting mold under the influence of a transverse, direct current magnetic field. *Metall. Materi. Trans. B*, 42(4):68–80, 2011.